Research Article **Open Access**

Kyriacos Neocleous*, Andreas Christofe, Athos Agapiou, Evagoras Evagorou, Kyriacos Themistocleous, and Diofantos Hadjimitsis

Digital mapping of corrosion risk in coastal urban areas using remote sensing and structural condition assessment: case study in Cyprus

DOI 10.1515/geo-2016-0063
Received Sep 29, 2015; accepted Jan 16, 2016

Abstract: Atmospheric corrosion is one of the main factors leading to performance deterioration of reinforced concrete buildings; and, hence, periodic structural condition monitoring is required to assess and repair the adverse effects of corrosion. However, this can become a cumbersome and expensive task to undertake for large populations of buildings, scattered in large urban areas. To optimize the use of available resources, appropriate tools are required for the assessment of corrosion risk of reinforced concrete construction. This paper proposes a framework for the production of digital corrosion risk maps for urban areas; Cyprus was used as a case study. This framework explored multi-temporal satellite remote sensing data from the Landsat sensors as well as corrosion risk factors derived from the results of a recently completed research project, entitled "STEELCOR". This framework was used to develop two corrosion risk scenarios within Geographical Information Systems, and to produce corrosion risk maps for three coastal cities of Cyprus. The thematic maps indicated that, for slight corrosion damage, the distance of reinforced concrete buildings from the coast was more influential than the building age. While, for significant corrosion damage, the maps indicated that the age of RC buildings was more influential than the distance from the coast.

Keywords: GIS; risk area; steel corrosion; reinforced concrete; satellite remote sensing; Landsat; classification; non-destructive testing; simplified damage index

1 Introduction

Concrete reinforced with steel rebars is used worldwide for the construction of residential and commercial buildings as well as public infrastructure, such as bridges and retaining walls. However, in due course, the performance of reinforced concrete (RC) will most likely deteriorate, mainly as a result of atmospheric corrosion of steel rebars [1]. This is an electrochemical process, initiated by the ingress of chlorides ions and/or carbon dioxide on the steel rebar's surface [2, 3]; its propagation in RC leads to the gradual formation of expansive oxide products and rust. The rate of corrosion in RC is influenced by internal and external factors, including material properties and environmental conditions [3]. It is typically faster in coastal areas, due to the high concentration of airborne chlorides in the environment and higher relative humidity. Furthermore, the corrosion rate also increases with atmospheric temperature (up to 40 degrees Celsius) [4].

Atmospheric corrosion in RC results to gradual mass loss of steel rebars and deterioration of their mechanical properties, as well as concrete spalling (*e.g.* Figure 1) and loss of bond between steel rebars and concrete [5–7]. As a result, the structural integrity and service life of RC reduce with time; for instance, the seismic fragility of RC structures increases as a result of atmospheric corrosion [8]. To mitigate the adverse effects of atmospheric corrosion, timely interventions should therefore be undertaken by owners/administrators of RC structures to repair the deteriorated structures and enhance their service life [9].

However, for administrators of large populations of RC structures (such as civil defense and/or municipal engineering departments), the assessment and repair of distress caused by corrosion can become a cumbersome and

***Corresponding Author: Kyriacos Neocleous:** Research Associate, Eratosthenis Research Centre, Department of Civil Engineering and Geomatics, Cyprus University of Technology, P.O.Box 50329, 3603 Lemesos, Cyprus; Email: Kyriacos.neocleous@cut.ac.cy, Tel. +357 2500 2005, Fax. +357 2500 2769

Andreas Christofe, Athos Agapiou, Evagoras Evagorou, Kyriacos Themistocleous: Research Associate, Eratosthenis Research Centre, Department of Civil Engineering and Geomatics, Cyprus University of Technology, P.O.Box 50329, 3603 Lemesos, Cyprus

Diofantos Hadjimitsis: Professor, Eratosthenis Research Centre, Department of Civil Engineering and Geomatics, Cyprus University of Technology, P.O.Box 50329, 3603 Lemesos, Cyprus

(a)

(b)

Figure 1: Distress caused by atmospheric corrosion of steel reinforcement in concrete elements: concrete spalling of (a) RC balcony slab and (b) RC columns at ground level.

expensive task to undertake, especially if their assets are scattered in large urban areas. Thus, to optimize the use of available resources (human, material and financial), appropriate tools are required to estimate efficiently the corrosion risk of RC structures in large urban areas. These tools could also form part of asset management systems typically used for the monitoring and repair of RC structures, such as Bridge Management Systems [10].

To develop an efficient corrosion risk assessment tool for RC construction, it is necessary to map the urban footprint expansion of the geographical area under examination. This could be achieved by utilizing satellite remote

sensing data, since these data were efficiently used to map urban areas as well urban sprawl of the last decades [11, 12]. As Nielsen [13] argues, remote sensing has the potential to collect information over large areas repeatedly, and monitoring urban land cover and land use changes [14, 15]. Therefore, remote sensing is suitable for investigating and evaluating models and hypotheses and for constructing new theories to help policy-makers and professionals. Reliable information regarding urban footprint can be retrieved from archive and current optical data and, hence, these could be used as a systematic tool for monitoring the structural condition of RC structures.

The main aim of our paper is the development of a cost-effective and simplified framework for the mapping of corrosion risk of RC buildings (located in coastal urban regions) by utilizing multi-temporal satellite remote sensing data and non-destructive test data of RC buildings, subjected to atmospheric corrosion. For demonstration purposes, the island of Cyprus was used as a case study, where thematic corrosion risk maps were successfully produced for three coastal cities.

2 Methodology

As shown in Figure 2, the proposed framework comprises of four interconnected steps, which can be applied to produce detailed corrosion risk maps of urban areas. Each step of the framework is outlined next as well as the application of the framework to our case study.

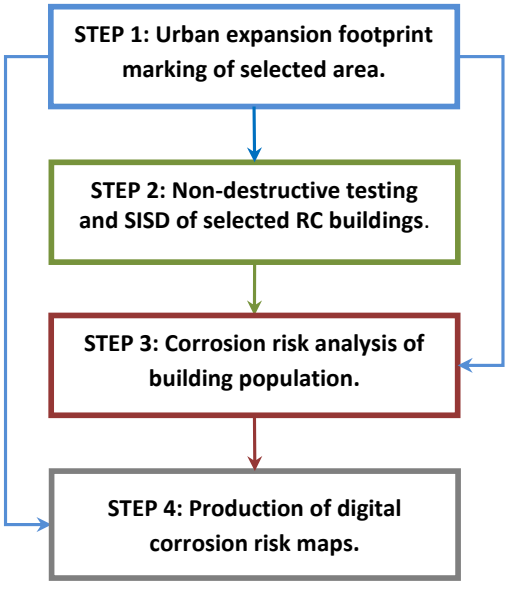

Figure 2: Proposed framework for the digital mapping of corrosion risk in coastal urban areas.

2.1 Urban footprint expansion

At the first step, we used medium spatial resolution images (30 metres pixel resolution) distributed freely from archive multispectral datasets, to detect the urban expansion footprint of the geographical area under consideration. The main purpose of this step was to classify different spatial zones according to the age of the building stock. To optimise the proposed framework, we focused on identifying built-up areas and zones rather than individual buildings. It should be noticed that, for our case study, remote sensing imagery was the only way to map urbanisation, since no government body in Cyprus has a relative geo-database to be used.

For our case study, five archive Landsat 5 TM, Landsat 7 ETM+ and Landsat 8 LDCM were used to mark the urban expansion footprint of the island. The overpass of the images was: 2013-05-31, 2009-09-25, 2002-08-13, 1990-08-04 and 1984-7-2; while the spatial resolution of these images was 30 metres in the visible and infrared part of the spectrum. All images were georeferenced into the WGS 84, 36N zone using ground control points obtained from cadastral maps.

After the necessary pre-processing analysis of the satellite data, including the radiometric corrections (*i.e.* reflectance at top of the atmosphere), we applied supervised classification using the ERDAS IMAGINE software. We have selected five main classes (Level 1) for the classification purposes: urban areas, vegetation, land and water; the fifth class was associated with un-classified pixels of the image. As indicated by current studies (*e.g.* [12]), Support Vector Machine (SVM) algorithms can achieve a high accuracy of classification results with kappa statistics more than 0.90. The SVM was also applied to the satellite imagery by using training areas, identified in the images. The SVM algorithm is a machine-learning technique that is well adapted to solve non-linear, high dimensional space classifications. SVM can be used for remote sensing applications, for classification of either multispectral or hyperspectral data, in which spectral separability is less than perfect [16]. The basic difference between SVM and other classifiers is the fact that SVM aims at identifying the boundaries between classes in n-dimensional spectral-space rather that assigning points to a class based on mean values. The final result of the SVM classifier is therefore a hyper-plane through n-dimensional spectral-space, which separates the different classes based on a

kernel function and parameters that are optimized using machine-learning to maximize the margin from the closest point to the hyper-plane.

In addition to the SVM classification, we applied Principal Component Analysis (PCA) transformation to compress the overall spectral information from the whole Landsat dataset (*i.e.* 2013-05-31, 2009-09-25, 2002-08-13, 1990-08-04 and 1984-7-2 image). PCA is a well-known orthogonal transformation where the initial information is re-projected into a new n-dimensional space of linearly uncorrelated variables. PCA transformation was applied to the whole multi-temporal dataset to detect any significant differences though out the years in the case study area. Areas that have changed (*i.e.* land use changes for instance rural areas to urban areas) can be easily detected in the 1st principal component of the transformation. The first PCA component has the largest possible variance of the data, and each succeeding component (*i.e.* PCA2, PCA3 etc.) has the highest variance possible under the constraint that it is orthogonal. Prior to the PCA transformation, all spectral bands were merged together in a single file. The first five bands of each image (visible RGB, near infrared NIR and middle infrared MIR) were combined together creating a new image with more than 25 different bands; this was followed by the PCA analysis.

2.2 Non-destructive testing

The second step comprised insitu visual examinations and non-destructive testing (NDT) of selected RC buildings using specialised NDT equipment (described in [17]) as well as the "CONTECVET Simplified" method, developed by the EC Innovation programme "CONTECVET" [18]. The CONTECVET method can be used for the quick and efficient structural condition assessment of a large number of RC buildings, subjected to atmospheric corrosion [9].

The main aim of this step was to assess the structural condition of RC buildings (located in the geographical area under consideration) by considering a range of building characteristics, such as environmental conditions, corrosion process characteristics and structural detailing of the steel rebars embedded in concrete. The final outcome of this step was the evaluation of the "Simplified Index of Structural Damage" (SISD) due to corrosion (for each RC structure examined). SISD is a simplified classification model, which considers two types of failure consequence: "Slight" and "Significant" [9, 18]. Slight failure consequence refers to corrosion induced distress that is either not serious or localised to the extent that a serious situation is not anticipated. Whilst significant failure consequence refers to the case where corrosion leads to serious distress of the RC structure, which can be a risk to life.

For our case study, we have initially undertaken visual examinations of 73 RC structures (mainly residential buildings), located in the coastal cities of Larnaca, Lemesos and Paphos. The results of the visual examinations were used to classify each RC structure in terms of exposure to environmental aggressivity (as defined by the European standard EN206, [19]) and type of distress, caused by corroded steel rebars (as defined by the CONTECVET method; see Table 1). The visual examinations were followed by comprehensive insitu NDT of 17 representative RC structures; our main selection criteria were distance from the coast and structural age. It is noted that the 17 structures were selected from the 73 visually examined structures. The NDT comprised mapping of the apparent corrosion in RC elements using the half-cell potential method [20], measurement of the electrical resistivity and insitu permeability of concrete [21], assessment of the carbonation depth by using the phenolphthalein solution method [22]. The concrete cover and steel rebar detailing were also assessed. Full details of the visual examinations and NDT programme are provided by Neocleous *et al.* [17].

The results of the NDT were then applied to the CONTECVET Simplified approach to classify the 17 RC buildings; the SISDs of these buildings ranged from medium to very severe (see Table 2).

2.3 Risk analysis of building population

At the third step of the framework, we have utilised the results of step 2 to derive corrosion risk factors for the two types of failure consequences (*i.e.* slight and significant damage). Thus, for our case study, we carried out a statistical analysis of available data, where the main parameters considered were the age of each building, its distance from

Table 1: CONTECVET distress levels due to corrosion of steel rebars in concrete.

Distress Type	Details
Level I	Rust spots from the corrosion products.
Level II	Concrete cracks (due to rebar corrosion) with width less than 0.3 mm
Level II	Concrete cracks (due to rebar corrosion) with width greater than 0.3 mm
Level IV	Spalling or loss of cover due to the pressure developed by the corrosion products

Table 2: Details of RC structures and their SISD determined using the CONTECVET approach.

Code	Building type	Construction date	Latitude	Longitude	Distance from coast	SISD*	
						Slight	Significant
103	Four storey RC hotel with infill masonry walls and stone	1977–1982	34°45’24.22"N	32°25’0.50"E	150	M	M
110	Football Stadium	2005+2010	34°44’37.15"N	32°26’22.59"E	750	N	M
111	Public Swimming Pool	2004	34°44’40.55"N	32°26’28.59"E	950	M	S
113	Ground floor RC house with infill masonry	2005	34°45’48.53"N	32°25’29.50"E	1150	M	S
121	Two storey public high-school with infill masonry walls	1990	34°45’25.10"N	32°27’13.58"E	2500	M	M
126	Ground floor RC house with infill masonry walls	1970	34°45’41.36"N	32°26’55.56"E	2800	S	V
127	Three storey residential RC building with infill masonry walls	2000	34°45’41.36"N	32°26’55.56"E	2800	M	M
128	Two storey RC building with infill masonry walls	1970	34°45’37.35"N	32°27’7.04"E	2850	M	S
132	Ground floor RC house with infill masonry walls in Geroskipou	1964	34°45’50.46"N	32°27’4.56"E	3100	M	S
204	Two storey RC building with infill masonry walls	1960	34°41’1.10"N	33° 3’28.09"E	75	S	V
208	Three storey RC offices building in Vassiliko Cement Factory	1960	34°43’20.82"N	33°19’1.33"E	400	M	S
212	RC Old Silos at Vassiliko Factory	1975	34°43’20.82"N	33°19’1.33"E	400	M	S
216	Two storey RC Municipal Health Services building with infill masonry walls and stone	1960	34°40’24.42"N	33° 2’20.09"E	410	S	V
226	RC house on pilotis	1990	34°40’51.47"N	33° 0’25.45"E	2700	M	M
227	RC ground floor house at Trachoni	1978	34°39’33.87"N	32°58’3.66"E	3800	S	V
228	Six storey RC building on pilotis	1985	34°40’50.28"N	33° 1’20.53"E	1700	Mm	S
229	Twelve storey RC building with basement	1980	34°39’53.04"N	33° 0’57.43"E	865	S	V

N: Negligible, M: Medium, S: Severe, V: Very severe

Table 3: Corrosion risk factors derived for coastal urban areas in Cyprus.

Construction Date	Distance from coast (metres)	Average slight risk	Average significant risk
Before 1984	0–500	M to S	S to V
Before 1984	500–1500	S	S to V
Before 1984	1500–3000	M	S to V
1984–1990	0 to 500	S	S
1984–1990	500–1500	M to S	S
1984–1990	1500–3000	M	S
1990–2000	0 to 500	M to S	M
1990–2000	500–1500	M to S	M
1990–2000	1500–3000	N to M	M
2000–2010	0 to 500	N	M
2000–2010	500–1500	N	M
2000–2010	1500–3000	N	M
After 2010	0 to 500	N	N
After 2010	500 to 1500	N	N
After 2010	1500 to 300	N	N

N = Negligible, M = Medium, S = Severe, and V = Very Severe

the coastline and extent of structural damage due to corrosion, *i.e.* distress type (based on the visual examinations) and the SISD classification. To simplify the risk analysis, risk factors were derived for specific building ages and spatial zones (as outlined in Table 3).

2.4 Production of corrosion risk maps

At the final step of our framework, the ArcGIS software was used to apply the derived corrosion risk factors to the various spatial zones, marked as urban areas in Step 1.

Since the main cities of the island are developed along the coastline, three different buffer zones were applied in the Geographical Information System (GIS) environment: from 0 to 500 metres, 500 to 1500 metres and 1500 to 3000 metres from the coastline. Furthermore, the urban areas, mapped at step 1 of the framework, were used to group the different building periods. The earliest image used here was from 1984 and, hence, the pixels classified as urban areas in the Landsat image of 1984 were considered as buildings constructed prior to 1984 (see Table 3). The new urban areas built between 1984 and 1990 were determined by excluding the pixels (classified as urban areas) of the 1984 image from the 1990 image. We have applied the same procedure to determine the urban areas built between 1990 and 2000, 2000 and 2010, 2010 and 20130. The two GIS layers (*i.e.* distance from the coastline and construction date) were then merged to identify the different construction periods in relation with their distance from the coastline. Then, the corrosion risk factors shown in Table 3 were applied to the various urban areas to produce the thematic maps.

3 Results

For each Landsat image, ground truth data were used from the image to train the SVM classifier. Homogeneous and representative areas of interest (AOI) for the different classes (*i.e.* urban areas, vegetation, land and water) were also selected for validation and accuracy assessment of the classification results. It should be noticed that, for the archive satellite data, sample AOIs from the historic centres of the coastal cities of Cyprus were used as ground truth, since no significant changes (*i.e.* land use changes) have occurred in these areas during the last decades. Figure 3 shows an example of the final classification analysis using the 2013 Landsat 8 LDCM image; urban areas are indicated with red colour. A 0.85 kappa value was obtained, indicating that we have achieved accuracy for the final classification of the entire dataset, providing in this way a reliable dataset for the next steps of the proposed framework.

The classification results from the Landsat imagery of Cyprus displayed a complex urban footprint of a coalescent urban core and a complex, sprawling suburban to splinter development in rural areas. As anticipated, urban areas in Cyprus were mainly marked in the coastal zone

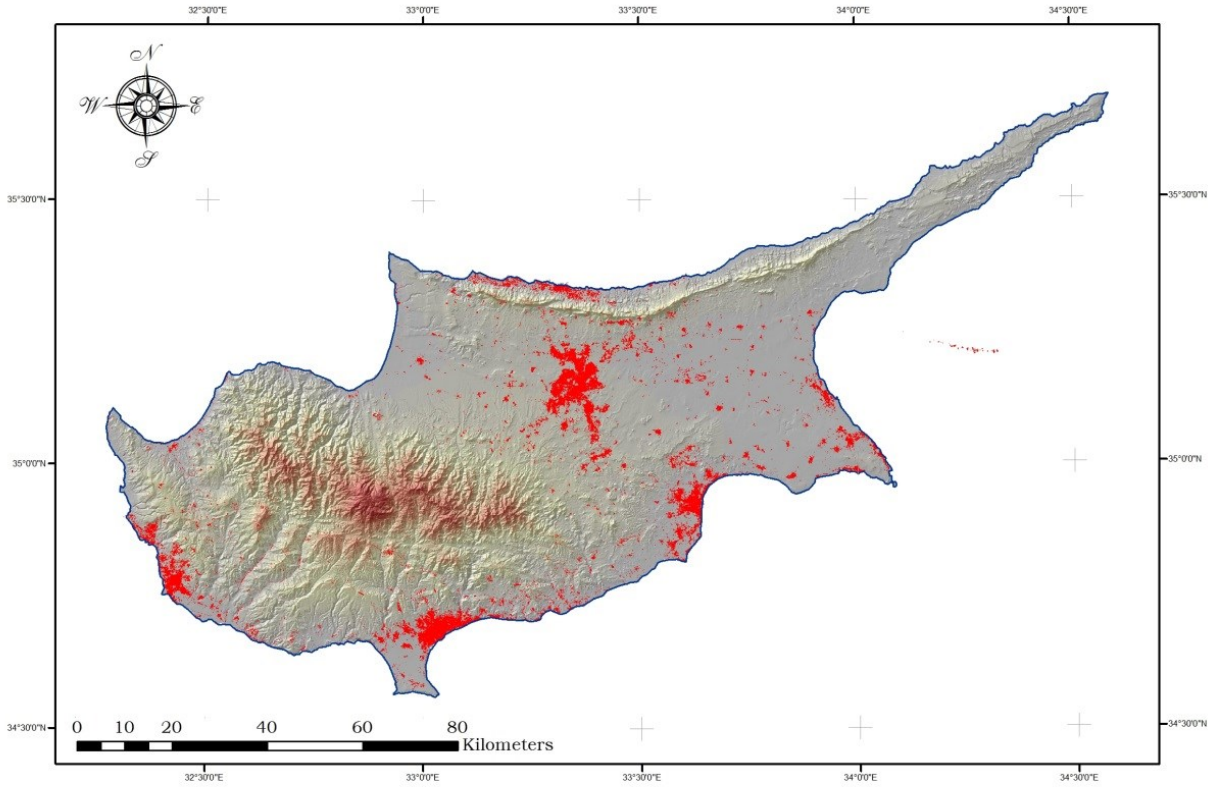

Figure 3: Urban areas (red colour) as classified using the 2013 Landsat 8 LDCM image.

of the island as well as to the city of Nicosia, located in the northern-central part of Cyprus. Figure 4 shows the results of the urban expansion footprint marking in Cyprus from the mid-1980s until 2013. Urban areas during the 1980's and 1990's are indicated in green and blue colour, respectively. Orange and red colours are used for areas urbanised during 2000-2010 and 2010-2013, respectively. The calculation of the total area of expansion of the urban areas between the different multi-temporal datasets was carried out through image subtraction analysis. The results are quite similar with other studies performed by the authors [12]. It is clear that the three coastal urban areas (*i.e.* cities of Larnaca, Lemesos and Paphos) have expanded mainly during the last 25 to 30 years, especially during the 1990's. The results of the urban expansion footprint indicated that urban areas have been expanded more than 300% for the period 1984–2013.

This observation is also recorded in the PCA analysis shown in Figure 5. As mentioned in the previous section, to apply this image processing, the dataset (1984–2013) was merged and then the PCA was applied to the entire dataset (including 25 spectral bands). The first principal component (PCA1) of this multi-temporal image, indicated with pink colour in Figure 5, indicates the most dramatic changes observed in this period. In addition to the urban expansion changes, other land use changes are also observed, such as vegetation covering soil areas. This however should be linked with the seasonal changes rather than real land use changes. The results from the PCA analysis are in line with the urban expansion, as recorded from the classification processing.

Figure 6 and 7 show the maps produced by applying the "Slight" and "Significant" risk factors respectively. In the case of slight corrosion risk scenario, the maps indicate that distance from the coast is generally more influential than the age of RC buildings. Figure 8 shows, for each city, the proportion of its urban area subjected to each type of "Slight corrosion" risk. It is clear that there is a negligible "Slight corrosion" risk for up to 50% of the structures located in the buffer zone under consideration (*i.e.* up to 3 km from the coastline). While another 40 to 45% of the structures have "Slight corrosion" risk equal or higher than "Medium". It is worth noticing, that Paphos has the highest proportion of urban area subjected to a Severe "Slight corrosion" risk; this is because Paphos was largely urbanised by the coastline, especially in the 1980s and early 1990s.

For the significant corrosion risk scenario, the maps (shown in Figure 7) indicate that the age of RC buildings is more influential than the distance from the coast. A higher

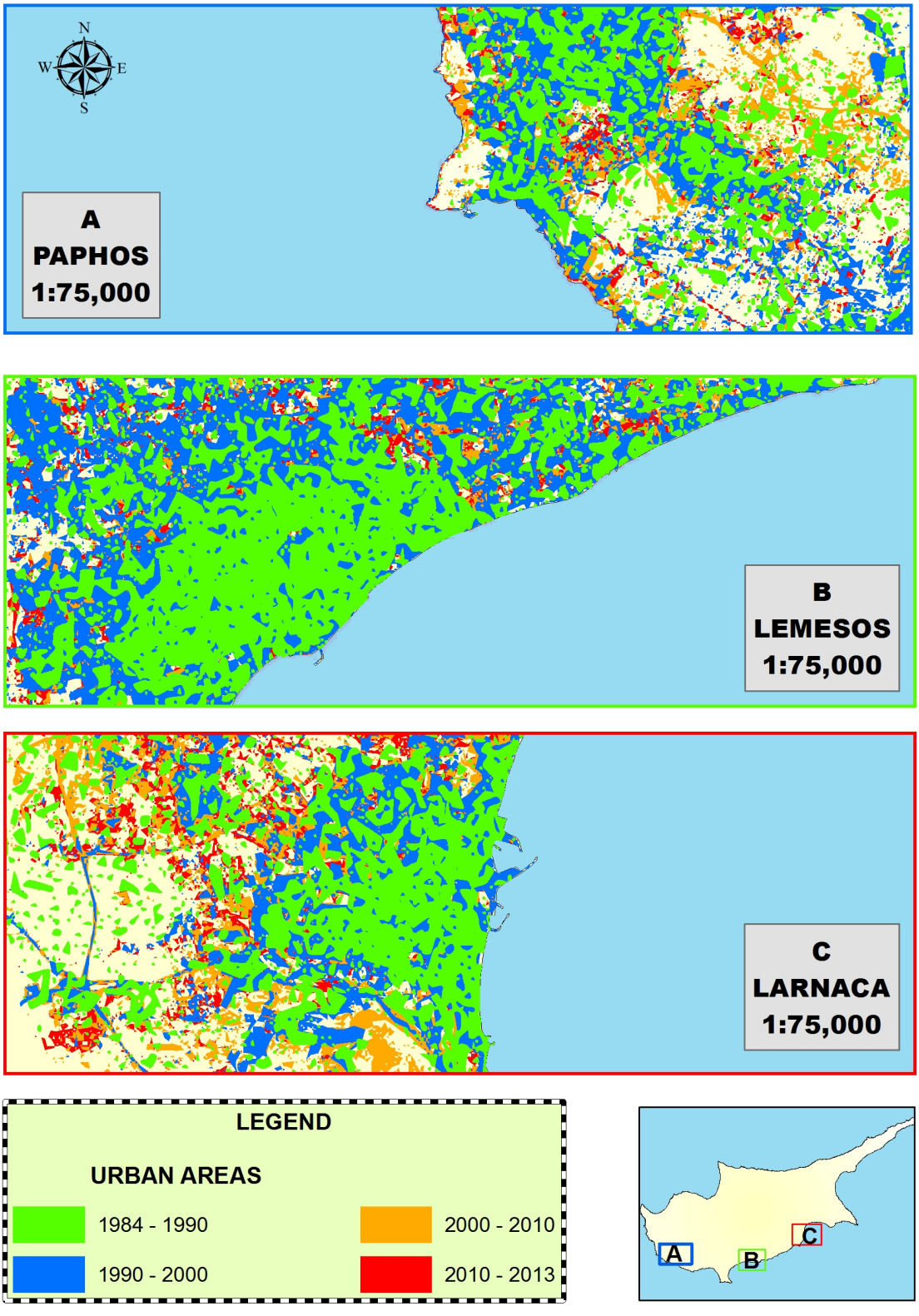

Figure 4: Expansion of urban footprint in Cyprus from mid-1980s until 2013.

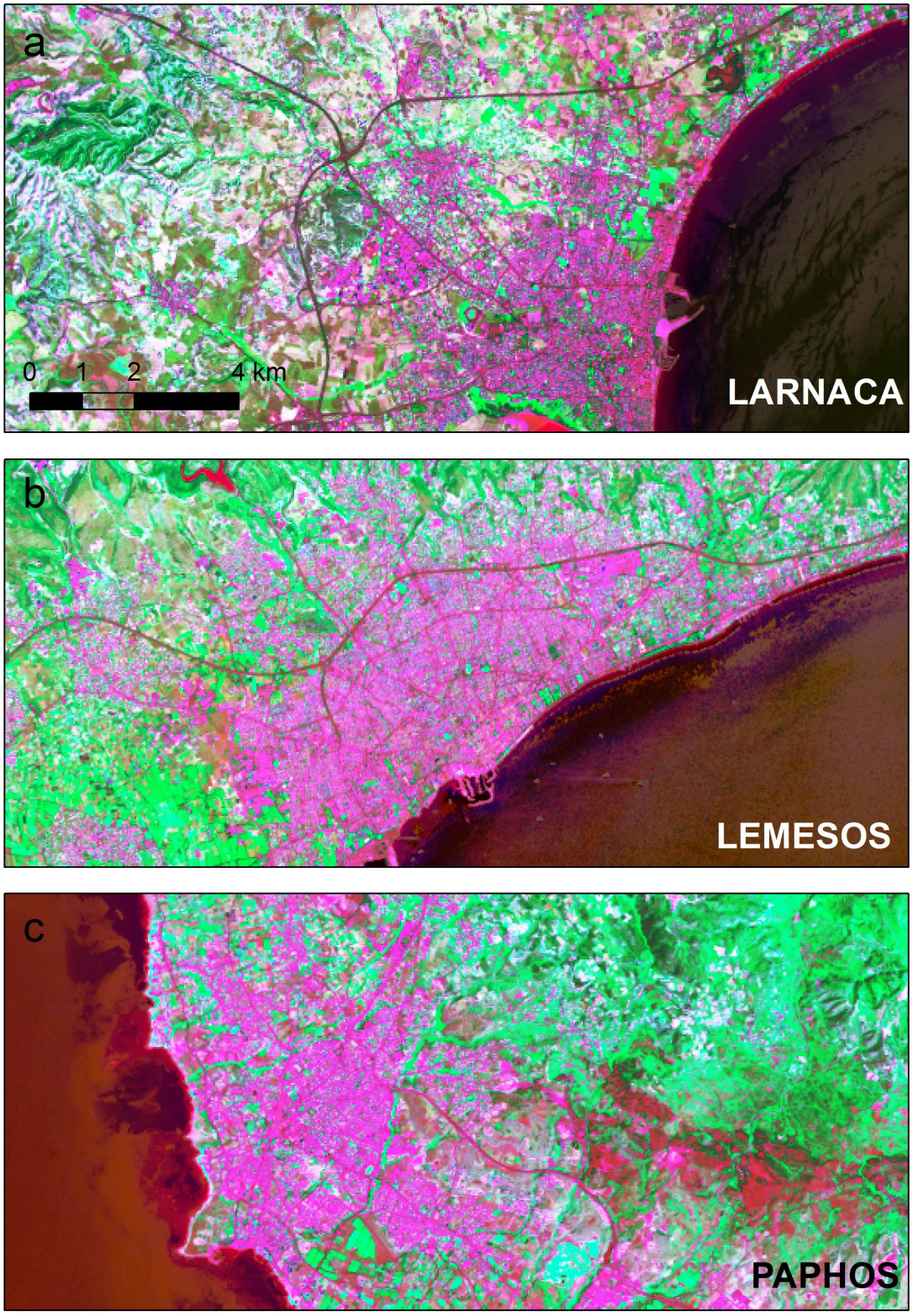

Figure 5: PCA transformation undertaken for the coastal cities of Larnaca, Lemesos and Paphos.

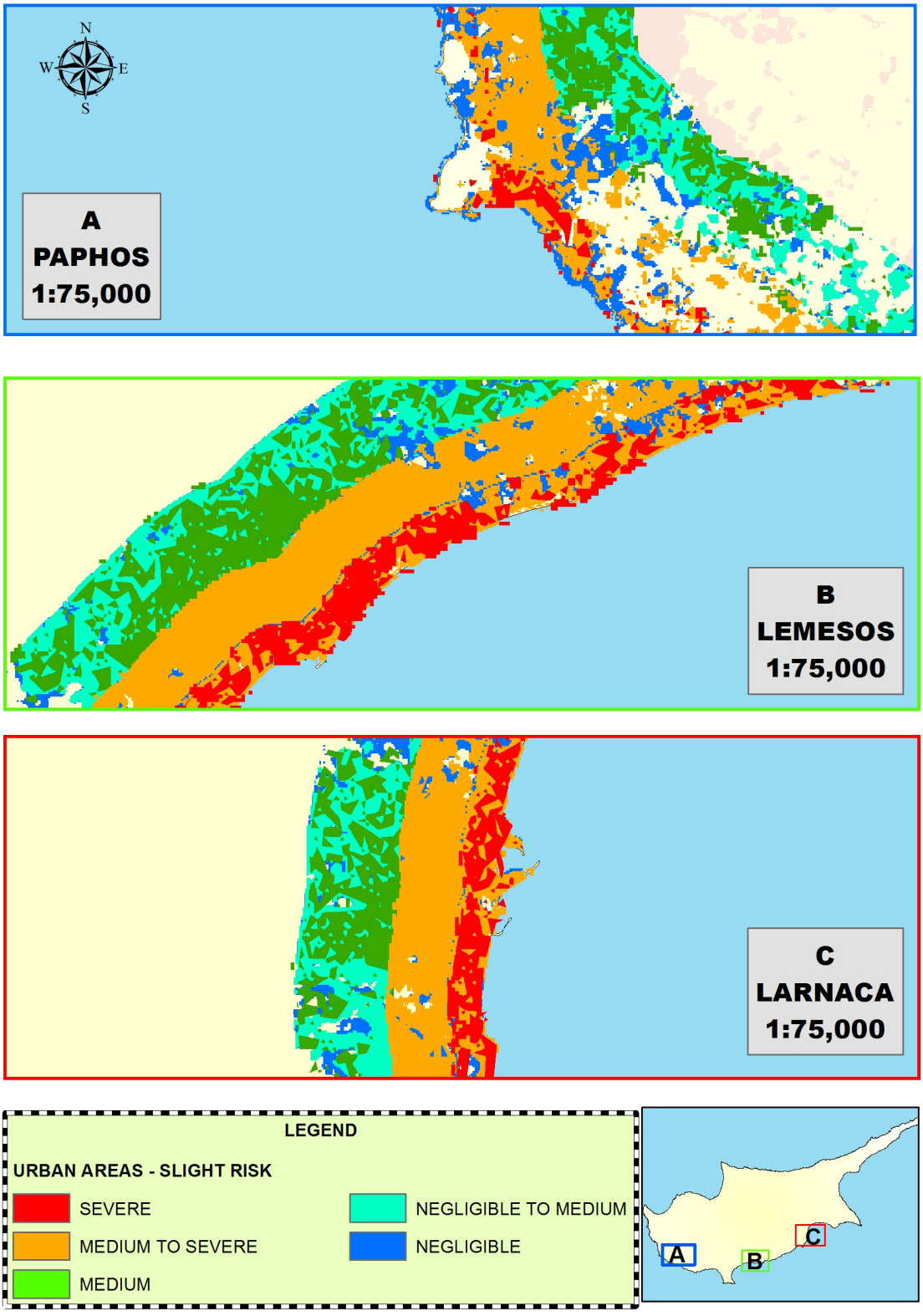

Figure 6: Slight risk due to steel corrosion in the coastal cities of Larnaca, Lemesos and Paphos (for a distance up to 3000 m from the coast).

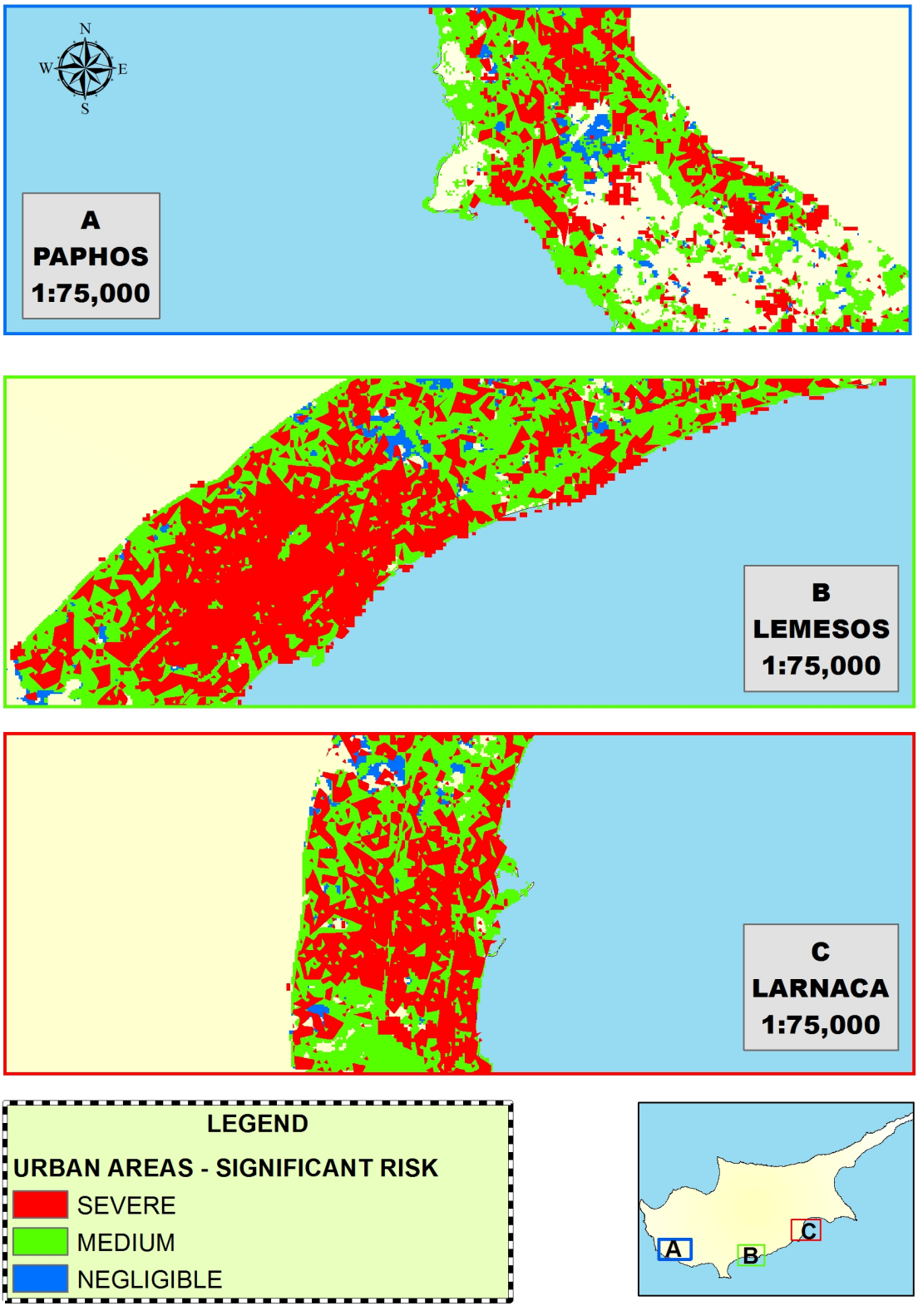

Figure 7: Significant risk due to steel corrosion in the coastal cities of Larnaca, Lemesos and Paphos (for a distance up to 3000 m from the coast).

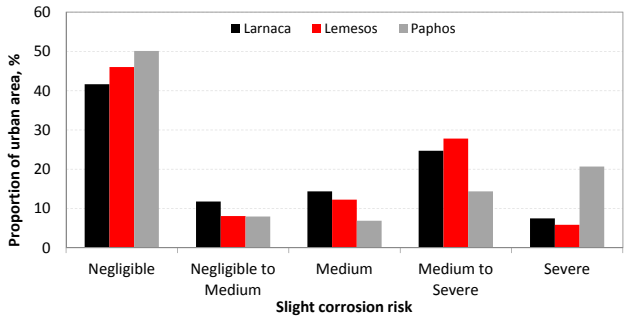

Figure 8: Proportion of urban areas subjected to each type of slight corrosion risk (for a distance up to 3000 m from the coast).

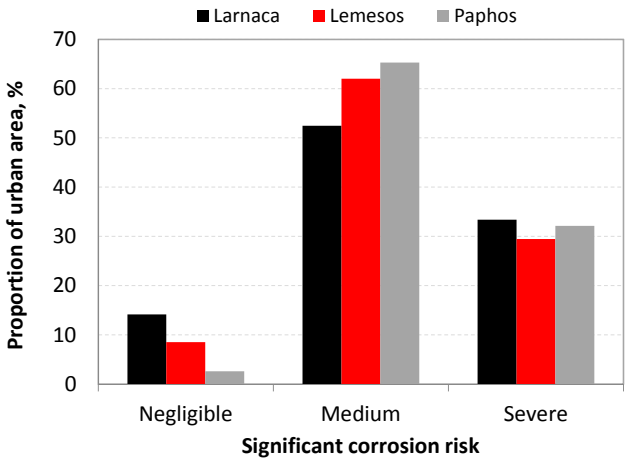

Figure 9: Proportion of urban areas subjected to each type of significant corrosion risk (for a distance up to 3000 m from the coast).

corrosion risk is observed for all three cities in the spatial zones where there are RC buildings; up to 90% of the urban areas are subjected to a "Significant corrosion" risk equal or higher than "Medium".

4 Discussion

We have proposed a framework for the digital corrosion risk mapping of RC structures in urban coastal areas. This framework utilised risk factors, derived from the structural condition assessment of representative RC buildings as well as satellite remote sensing data, obtained for the last 30 years. The proposed methodology can be applied by stakeholders to estimate, for large urban areas, the problem related with corrosion of RC structures. Furthermore, the proposed methodology can be part of an integrated asset management system where the main target will be to optimise the repair and maintenance costs of RC structures.

The semi-automatic extraction of urban areas using classification processing with high accuracy (*i.e.* Kappa statistics) is a useful tool for mapping building areas and zones of different construction periods. As demonstrated here, satellite data can be used to map the urban areas for different periods and therefore provide a reliable and accurate dataset for corrosion risk mapping purposes at the regional level. The relative low cost of satellite datasets (or as in our case where Landsat series are freely distributed by USGS) can provide an alternative way of digitizing the urban footprint of large geographical areas compared to other techniques, such as digitization of local cadastral maps. It should be mentioned that these maps do not have a complete record of buildings, but changes in land distribution. Using higher spatial resolution images, with less than 2 metres pixel size (such as IKONOS, GeoEye, Pleiades, WorldView), stakeholders can even map individual buildings or blocks; and this can potentially provide the means for more detailed corrosion risk mapping. For instance, this option can be used for a population of RC structures scattered in a relatively small geographical area, or when considering the corrosion risk of important RC structures, such as hospitals, schools and utility buildings. It should be noticed though that such images are accessible since 1999 and, this can be a limiting factor for the proposed framework; higher costs and processing time are also limiting factors for using high resolution images.

The framework was applied for two corrosion risk scenarios (*i.e.* for slight and significant risk) to produce detailed corrosion risk maps for the three main coastal cities of Cyprus (*i.e.* Larnaca, Lemesos and Paphos). The "Slight risk" maps indicate that distance from the coast is more influential than the age of RC structures, since this risk type considers structural damage caused by localised depassivation of the steel rebars (as a result of the ingress of airborne chlorides [2]). Whilst the "Significant risk" maps indicate that the age of RC structures is more influential than the distance from the coast. This is because the "Significant risk" considers corrosion that reached its propagation stage, where rust and oxide products are considerably produced along the length of the steel rebar, leading to concrete spalling and mass loss of the steel reinforcement. Our findings from the visual examinations and non-destructive testing of RC buildings support these remarks. A higher degree of structural damage due to corrosion is observed in older RC buildings (irrespective of their distance from the coast), especially in cases where there was limited maintenance and/or areas of high water concentration (such as unprotected roofs or septic tanks). Thus, to minimise the risk of structural damage due to corrosion, it is essential that critical RC elements (especially exter-

nal columns, beams and slabs) have low permeability and sufficient concrete cover which is in-line with the recommendations of Eurocode-2 [23]. In addition, durable water proofing should be applied to RC elements, exposed to high concentrations of water and humidity.

Acknowledgement: This research was funded under "Desmi 2009-2010" for research, technological development and innovation, which was co-financed by the European Regional Development Fund and the Cyprus Research Promotion Foundation (contract NEA ΥΠΟΔΟΜΗ/ΝΕΚΥΠ/0311/29).

References

[1] Schiessl P. Corrosion of steel in concrete: report of the Technical Committee 60 CSC, RILEM (the International Union of Testing and Research Laboratories for Materials and Structures), International Union of Testing and Research Laboratories for Materials and Structures. Technical Committee 60–CSC., 1988

[2] Montemor MF, Simões AMP, Ferreira MGS. Chloride–induced corrosion on reinforcing steel: from the fundamentals to the monitoring techniques. Cement and Concrete Composites, 2003, 25, 491–502

[3] Ahmad S. Reinforcement corrosion in concrete structures, its monitoring and service life prediction – a review. Cement and Concrete Composites, 2003, 25, 459–71

[4] Alhozaimy A, Hussain RR, Al–Zaid R, Al–Negheimish A. Coupled effect of ambient high relative humidity and varying temperature marine environment on corrosion of reinforced concrete. Constr Build Mater, 2012, 28, 670–9

[5] Apostolopoulos CA, Demis S, Papadakis VG. Chloride–induced corrosion of steel reinforcement – Mechanical performance and pit depth analysis. Constr Build Mater, 2013, 38, 139–46

[6] Apostolopoulos CA, Michalopoulos D, Koutsoukos P. The Corrosion Effects on the Structural Integrity of Reinforcing Steel. J of Materi Eng and Perform, 2008, 17, 506–16

[7] Demis S, Pilakoutas K, Apostolopoulos CA. Effect of corrosion on bond strength of steel and non–metallic reinforcement. Materials and Corrosion, 2010, 61, 328–31

[8] Pitilakis KD, Karapetrou ST, Fotopoulou SD. Consideration of aging and SSI effects on seismic vulnerability assessment of RC buildings. Bulletin of Earthquake Engineering, 2014, 12, 1755–76

[9] fib CEB–FIP. Bulletin 62: Structural Concrete – Textbook on behaviour, design and performance, fib CEB–FIP, 2012

[10] Mirzaei Z, Adey BT, Klatter L, Thompson PD. The IABMAS bridge management committee overview of existing bridge management systems 2014, International Association for Bridge Maintenance and Safety – IABMAS, 2014

[11] Hegazy IR, Kaloop MR. Monitoring urban growth and land use change detection with GIS and remote sensing techniques in Daqahlia governorate Egypt. International Journal of Sustainable Built Environment, 2015, 4, 117–24

[12] Agapiou A, Alexakis DD, Lysandrou V, Sarris A, Cuca B, Themistocleous K et al. Impact of urban sprawl to cultural heritage monuments: The case study of Paphos area in Cyprus. Journal of Cultural Heritage, 2015,

[13] Nielsen MM. Remote sensing for urban planning and management: The use of window–independent context segmentation to extract urban features in Stockholm. Computers, Environment and Urban Systems, 2015, 52, 1–9

[14] Alexakis DD, Agapiou A, Hadjimitsis DG, Retalis A. Optimizing statistical classification accuracy of satellite remotely sensed imagery for supporting fast flood hydrological analysis. Acta Geophysica, 2012, 60, 959–84

[15] Alexakis DD, Hadjimitsis DG, Agapiou A, Themistocleous K, Retalis A. Monitoring urban land cover using satellite remote sensing techniques and field spectroradiometric measurements: case study of "Yialias" catchment area in Cyprus. APPRES, 2012, 6, 063603–

[16] Heumann BW. An object–based classification of mangroves using a hybrid decision tree–support vector machine approach. Remote Sensing, 2011, 3, 2440–60

[17] Neocleous K, Christofe A, Hadjimitsis D. NDT Assessment of The Selected Buildings, Cyprus University of Technology, Limassol, 2014

[18] Rodriguez J, Andrade C. CONTECVET A validated users manual for assessing the residual service life of concrete structures, England, 2000

[19] European Committee for Standardization. EN 206 Concrete – Specification, performance, production and conformity, CEN, Brussels, 2013

[20] ASTM International. Standard test method for Corrosion Potentials of Uncoated Reinforcing Steel in Concrete, West Conshohocken, 2009

[21] Torrent R, Denarié E, Jacobs F, Leemann A, Teruzzi T. Specification and site control of the permeability of the cover concrete: The Swiss approach. Materials and Corrosion, 2012, 63, 1127–33

[22] RILEM TC56. CPC–18 Measurement of hardened concrete carbonation depth. Materials and Structures, 1988, 21, 453–5

[23] European Committee for Standardization. EN 1992-1-1 Eurocode 2: Design of concrete structures – Part 1-1: General rules and rules for buildings, CEN, Brussels, 2004